A NEW UNIVERSAL WORKABILITY CRITERION TO PREDICT THE INTERNAL AND EXTERNAL DUCTILE FAILURE IN COLD HEADING PROCESS

[1]AMAR SABIH, [2]JAMES NEMES

McGill University & Concordia University, Penn State University
E-mail: [1]amar.sabih@mcgill.ca, [2]jan16@psu.edu

Abstract - The occurrence of internal and external ductile failure in cold-headed products presents a significant obstacle in the fast-expanding cold heading (CH) industry. The presence of these types of ductile failure in cold-headed products may lead to catastrophic fractures under tensile loads even though the ductile nature of the material. Hence, several workability criteria were presented in the literature to predict each of the two failure types independently.
This paper presents the comprehensive experimental, metallurgical, and finite element simulation study of the internal and external ductile failure of the cold heading process (CHP) of 1038 steel. The outcomes of this study uncovered a new universal workability criterion that is suitable to predict internal and external ductile failures. The new workability criterion uses the stress triaxiality history as a damage parameter to accurately indicate the locus of initiation of the internal and external failures. Implementing the new universal criterion in the cold heading processes stages design will be a powerful tool to produce high-quality cold-headed products.

Keywords - Adiabatic Shear Band, Cold heading, Cracks, Ductile failure, Workability criterion.

I. INTRODUCTION

The cold heading process (CHP) is used to produce a large variety of components such as fasteners, studs, small shafts, and other machine parts. The CHP is a complicated process where the product quality relays on the complex interplay of material and process parameters. This process is currently one of the most important metal forming processes because of its many advantages over machining of the same part, including high productivity, complex final shapes, and minimum material waste. The CHP, which is a multistage forming process performed without an external heat source, involves applying a force to the free end of a metal workpiece. It is important to highlight that the designs of multiple stages of the cold-headed process are based on a large number of rules of thumb and trial and error expertise developed over many decades [1].
The cold heading industry is pushing toward faster headers, reducing the number of heading stages, and producing high-strength fasteners without heat treatment. To accomplish these goals, modified process designs are required, resulting in higher strains and strain rates. Unfortunately, the well-known CH rules of thumb failed to produce defect-free products manufactured under high strains and strain rates.
Okamoto et al. [2] classified cracks found in cold forging operations into two types, external and internal cracks. The first is the external oblique or longitudinal crack (α-type cracks) ([3], [4] (Fig 1. a); the second is the internal crack was identified as Θ-type is caused by the adiabatic shear band (ASB) phenomenon [1], which sometimes results in splitting of the heads of the fasteners [2], as shown in Fig. 1.b.
Longitudinal external cracks are parallel to the axis of the product and can run the full length. These cracks can also be due to the exhaustion of material ductility and that the plastic Limits of the material have been exceeded [5]. Oblique defects are typically characterized by a 45° shear crack in the upset portion. The presence of such a defect is indicative of localization due to flow softening. Flow softening may be caused by such factors as deformation heating, high friction and die misalignment that leads to higher stress concentration on the equatorial surface of cold-headed specimens [3], [6].
Oblique external defects are typically characterized by a 45° shear crack on the equatorial surface of a cold-headed specimen. The presence of such a defect may be attributed [6] to friction, which leads to non-uniform deformation and bulging of the surface. It may also be attributed ta the depletion of strain-hardening capacity due to deformation heating (flow softening), a chain of events that leads to higher concentrated strain on the equatorial surface of a cold-headed specimen [3].

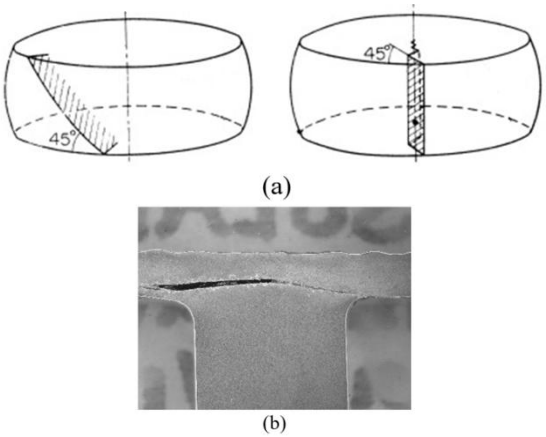


Fig. 1 (a) Schematic representation of external oblique and longitudinal fracture surface of upsetting specimen (adopted from Kudo and Aoi, 1967), (b) An internal crack in a cold-headed bolt caused by ASB phenomenon.

The internal ductile cracks in the CH process are usually developed within highly deformed adiabatic shears bands. An ASB is a narrow, nearly planar or two-dimensional region of very large shearing that sometimes occurs in metals and alloys as they experience intense dynamic loading (as in the CHP). Once the band is fully formed, the two sides of the region are displaced relative to each other [1], [7], [8], [9].

The formation of ASBs commonly occurs by impact loading at high strain rates (higher than 102 s-1) and high strains. The thickness of the most heavily sheared region may be a few tens of microns or less, and its length might extend many millimeters or centimeters [7].

At the early stages of deformation, the work hardening mechanism dominates over the thermal softening mechanism causing an increase in the flow stress. However, most of the plastic work (90-95%) is converted into heat causing a local temperature to increase and flow stress to decrease. Thus, a competing mechanism between the work hardening and the thermal softening starts and continues in the deformation zone. If the material deformation continues long enough; the thermal softening mechanism dominates over the work hardening, triggering unstable deformation. This instability will force the deformation to localize into a narrower band. As a result, plastic deformation leads to a self-sustaining cycle of instability: Inhomogeneous plastic shear flow ➔ non-uniform temperature distribution ➔ local thermal softening and further inhomogeneous shear plastic flow. The result is the formation of a highly localized shear band. The continuous localization may lead to final ductile failure [7], [10], [11], [12].

The ductile failure caused by the ASB is due to the void nucleation and coalescence inside the highly localized band. Even if the band does not fracture, it retains a weak or brittle microstructure and a preferable fracture path in the middle of the ductile matrix [13].

II. OBJECTIVE

Many researchers [3], [14], [15], focused on external defect type and provided criteria to predict it. On the other hand many researchers studied the internal ductile cracks within shear bands and reported that internal defects occur within the shear band and become the sites of eventual failure. Moreover, they presented different criteria to predict this type of defect [1], [2], [16]-[21].

The objective of this study is to develop a universal workability criterion using DWCT to predict external and internal ductile defects (cracks).

III. REVIEW OF DUCTILE FRACTURE CRITERIA

The ductile damage and fracture process involves several metallurgical events involving different steps between micro-void nucleation and cracks propagation. The initial phase of damage coincides with void nucleation at inclusion edges or grain boundaries due to the interaction of local stresses and dislocations phenomena. The damage in the material is then driven by the accumulated plastic strain and affected by the stress triaxiality. Stress triaxiality is defined by the dimensionless parameter ($\sigma_m/\bar{\sigma}$) where σ_m is the mean stress or the hydrostatic stress and $\bar{\sigma}$ is the equivalent stress. Moreover, deformation under compressive loads shows that when there is negative stress triaxiality (within the ASB), the formability is greater than in the tensile loading state (in case of external fracture), i.e. positive stress triaxiality [22]. It is therefore competition between the stress triaxiality levels reached in the specimen and the high plastic strains, which determine the failure site [15].

Gouveia et al. [23] and Shivpuri [24] concluded that Oyane's criterion [25], which is based on the void growth model and the theory of porous plasticity, was the best among the criteria considered in their work in terms of modelling the prediction of free (external) surface fracture initiation.

Oyane and his colleagues [26] employed the history of stress triaxiality and equivalent plastic strain to formulate their criterion to predict fracture at the external free surface in upsetting. This criterion states that ductile failure initiation takes place when the accumulated equivalent plastic strain, with the stress triaxiality as a weighting function, reaches a certain limit. This criterion is widely used because of its simplicity and capability in predicting fractures in different types of metal-forming processes. However, all Oyane criterion applications in the literature are limited to external fracture. The tensile character of the stress triaxiality on the equatorial surface of a cold-headed specimen makes it a candidate for insertion into a ductile fracture criterion such as the Oyane criterion. In this case, the contribution of this parameter to fracture is similar to that of the hoop stress [3].

In the available literature, the only usage of this criterion to study internal ductile failure under compressive loads was by Shin and Kawai [27], [28]. They used the Oyane criterion to study and compare the damage inside cold-headed cylindrical specimens of different aspect ratios and by using conical dies with different angles.

Based on the successful results of using the criterion introduced by Oyane [25] in predicting the ductile failure initiating under compressive and tensile loads (positive and negative stress triaxialities), this work will employ this criterion as a universal workability

criterion for internal and external ductile failure in CHP.

Oyane et al. [26] proposed a criterion which predicts failure in different types of metal forming processes. This criterion is based on the damage estimated by the history of the equivalent plastic strain and stress triaxiality, expressed as a weighting function. The basic mathematical expression for the ductile fracture criterion is:

$$\int_0^{\bar{\varepsilon}^f} \left(1 + A\frac{\sigma_m}{\bar{\sigma}}\right) d\bar{\varepsilon} = B \qquad (1)$$

which can be written as:

$$\bar{\varepsilon}^f = B - A\int_0^{\bar{\varepsilon}^f} \frac{\sigma_m}{\bar{\sigma}}\, d\bar{\varepsilon} \qquad (2)$$

where A and B are material constants . $\bar{\varepsilon}^f$ is the equivalent strain to fracture. The integral part in Equation (2) is called the "damage indicator" [29].

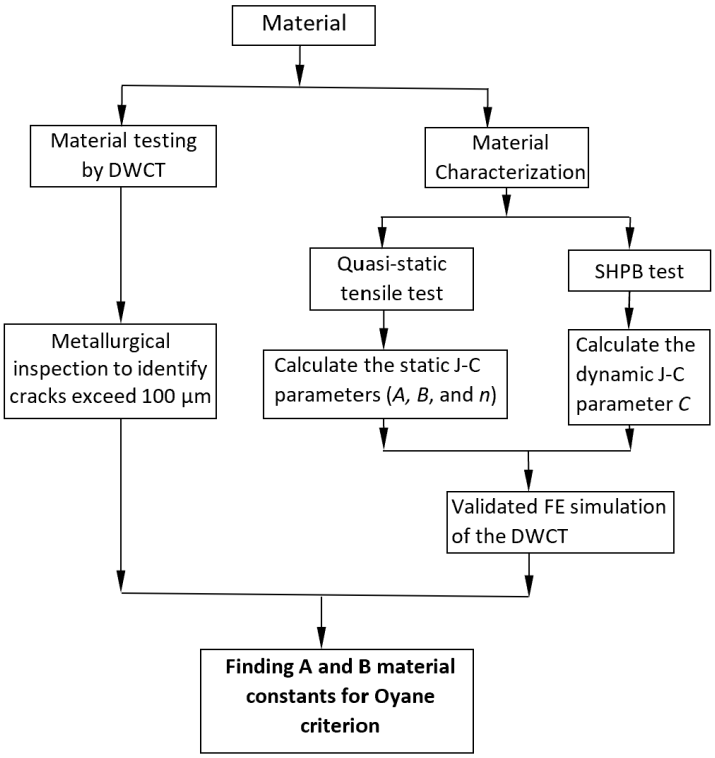


Fig. 2 The methodology to determine the material parameters for the workability criterion

This indicator can be calculated by integrating the stress triaxiality history with respect to equivalent strain. This criterion is widely used because of its simplicity and capability to predict failure in different types of metalworking processes.

IV. METHODOLOGY

The methodology to determine the material parameters for the workability criterion employs several steps presented in Fig. 2. These steps consist mainly of the drop weight compression test (DWCT) to simulate the CHP in conjunction with finite element analysis (implemented within ABAQUS/Explicit). Metallographic inspection for the deformed specimens is performed to locate the failed zones inside the ASB. The experimental and finite element simulation results are used to find the material constants for the Oyane Criterion. The failure measure in this work is taken to be the appearance of the external oblique and longitudinal cracks and internal cracks along the ASB that exceed 100 µm in length.

A. Experimental and FE Modelling

A.1 Testing Material

The 1038 steel chemical composition in weight percent of 0.038% C, 0.82% Mn, 0.19% Si, 0.001% Mo, 0.002% S, 0.003% Sn, 0.007% P, 0.08% Cr, 0.003% Al, 0.08% Ni, 0.005% V, 0.0044% N, 0.0001% B and 0.04% Cu.

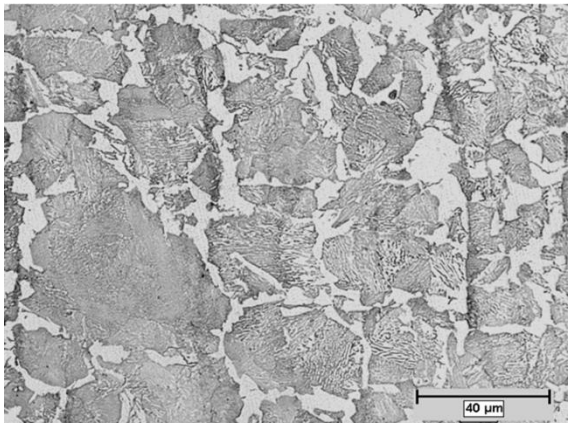


Fig. 3 1038 steel microstructure

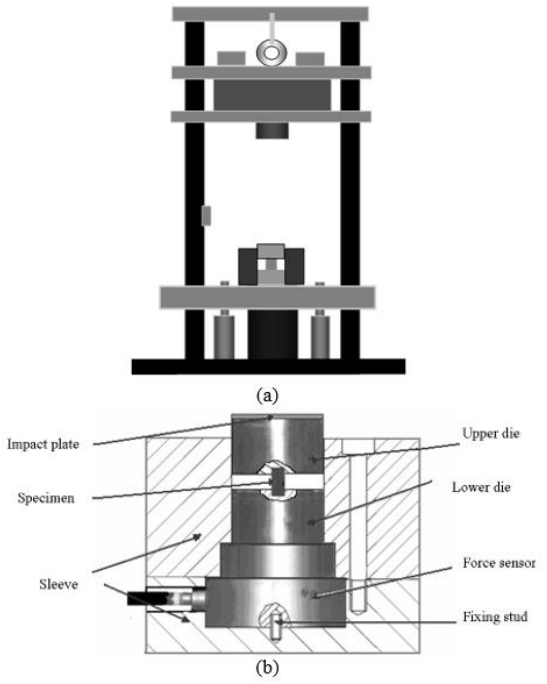


Fig. 4 (a) Schematic of the DWCT machine and (b) the specimen in the DWCT die arrangement

The microstructure consists of 50% ferrite matrix and 50% lamellar pearlite (Fig. 3)

A.2 Drop Weight Compression Test (DWCT)

The DWCT as described by Nickoletopoulos [3] was used as a workability test to perform the cold heading of the specimens (Fig. 4). The DWCT facilitates the testing of the CHP and it is capable of generating internal and external cracks during upset testing. The DWCT machine (Fig. 4-a) consists of a tower enabling interchangeable weight plates to be dropped from heights up to 2.4 m. The die set configuration (Fig. 4-b) rests on a central column that is welded to the base of the DWCT machine. Specimens for CH were machined with a tolerance of 0.02 mm from as-rolled rod material to a cylindrical configuration of 5.3 mm in diameter with aspect ratios of 1.6 and 1.8. A series of tests is performed by varying the weights until external and/or internal fracture is determined.

A.3 Finite Element Simulation and Constitutive Model

The finite element model (implemented with ABAQUS/Explicit) has been used to simulate the DWCT for the current work. The Johnson-Cook model (J-C) [30] is used to describe the thermo-plastic, rate-dependent behavior of the material in a two-dimensional, axisymmetric, adiabatic, analysis of a cylindrical specimen under impact loading. The meshing of the specimen is performed using 4-noded continuum elements with reduced integration and hourglass control (CAX4R).

The Johnson-Cook [30] model is used in these finite element simulations because it provides a reasonably good prediction for high-rate deformation mechanical behavior. This model is utilized extensively for computational purposes because it also contains parameters that are relatively easy to determine. Many researchers have reported satisfactory results using the JC model [31], [32].

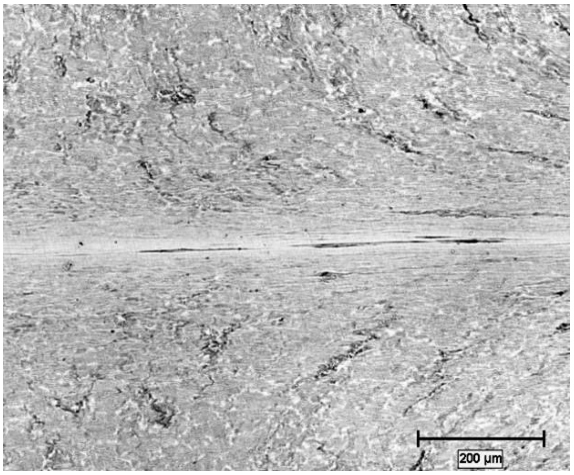


Fig. 5 Elongated cracks along a localized ASB in 1038 steel (aspect ratio= 1.8, drop height= 2.4 m, drop weight= 30.5 kg) (etchant: 2% Nital solution)

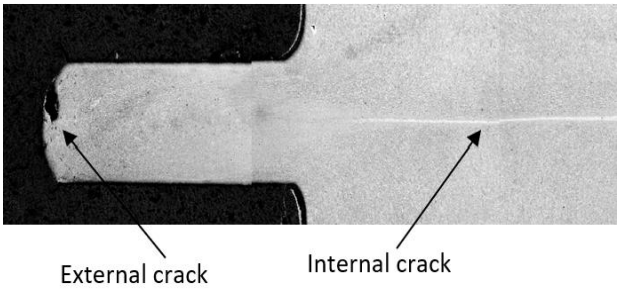


Fig. 6 DWCT specimen with internal and external cracks.

(Aspect ratio of 1.8, drop height of 2.4 m and drop weight 23.5 kg). (Le Pera's etchant: mixture of 1 g sodium metabisulfite + 100 ml water + 4 g of picric acid and 100 ml ethanol),

In the Johnson-Cook model, the Von-Mises flow stress is represented by a multiplicative relation as follows:

$$\bar{\sigma} = (A + B\bar{\varepsilon}_p^{\,n})(1 + C\ln\frac{\dot{\bar{\varepsilon}}_p}{\dot{\bar{\varepsilon}}_o})(1 - T^{*m}) \quad (3)$$

Where $\bar{\sigma}, \bar{\varepsilon}_p$ and $\dot{\bar{\varepsilon}}_p$ are the effective flow stress, the effective plastic strain, and the effective plastic strain rate respectively. $\dot{\bar{\varepsilon}}_o$ is normally taken to be 1.0 s^{-1}. *A, B, n, C,* and *m* are material constants and T^* is the normalized temperature. The first term characterizes the strain hardening, whilst the second part accounts for strain rate dependence, and the last term captures the temperature effects.

A.4 Finding Johnson-Cook parameters

The Split Hopkinson Pressure Bar (SHPB) is used to determine material response when subjected to deformation at high strain rates. Developed by Kolsky [33], the SHPB test has subsequently been used as a

dependable method for determining the material behavior at high strain rates that cannot be reached by traditional equipment such as hydraulic or screw-driven testing machines. Several SHPB tests were conducted on 5x5 mm cylinders to determine the dynamic J-C parameter (C) and it was found to be 0.1. On the other hand, the quasi-static tensile tests were performed on standard specimens to determine the J-C static parameters (A, B and n) and were determined to be 420 MPa, 1350 MPa, and 0.63, respectively.

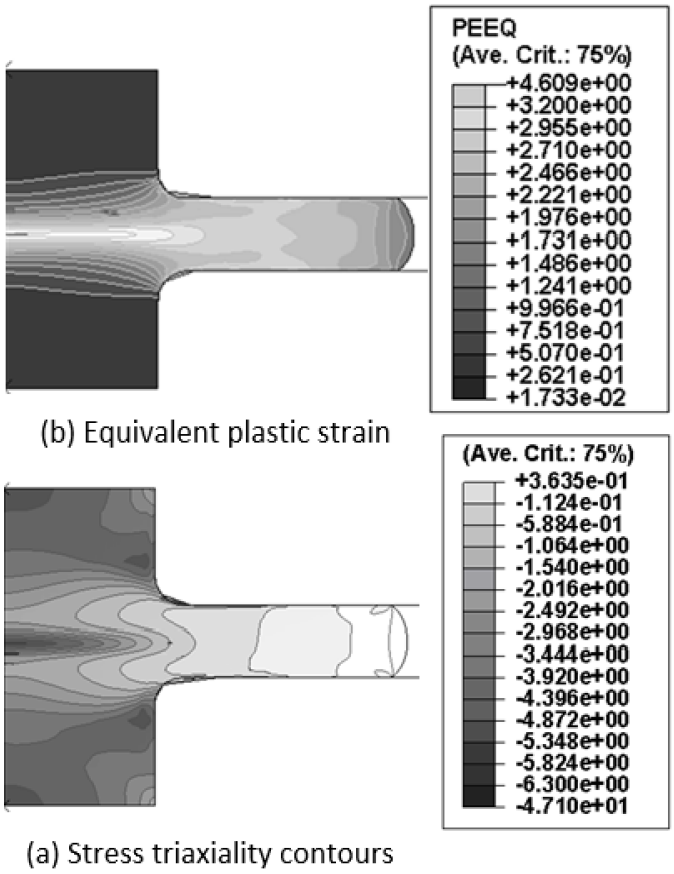


Fig. 7 Finite element contours: (a) stress triaxiality, (b) equivalent plastic strain

The thermal softening constant, m, was set at 1.00, which has been reported to be a good approximation for several metals [30].

V. RESULTS AND DISCUSSION

In general, microscopic and metallurgical examination of the DWCT specimens at different levels of deformation showed that voids and cracks that exceed 100 µm were found along the ASBs inside DWCT specimens (Fig. 5). Moreover, longitudinal external cracks that exceed 100 µm were noticed in some DWCT specimens (Fig. 6)

Finite element simulation runs were performed for the DWCT tests taking into account the different dropped weights used. Simulation results were used to study the changes in stress triaxiality and equivalent plastic strain at different locations of the specimens. The finite element simulation results of the equivalent plastic strain and stress triaxiality contours for a DWCT specimen are shown in Fig. 7.

The material constants of the ductile fracture criterion were determined in several steps by combining the results of the metallographic inspection and the FE simulation runs for the series of DWCTs. The first step is to indicate the position of each internal or external crack that exceeds 100 µm in length. Using the FE simulation contours for each DWCT specimen, the elements that correspond to the failed locations on the DWCT specimen were indicated. This was followed by determining the time history of the equivalent stress, the equivalent plastic strain and the hydrostatic pressure for these elements to be used in finding the material parameters for the criterion.

For these failed locations, the $\bar{\varepsilon}_p^f$ and $\int_0^{\bar{\varepsilon}_p^f} (\sigma_m / \bar{\sigma})\, d\bar{\varepsilon}_p$ values will be calculated from the FE simulations of the corresponding specimens. The relationship between $\int_0^{\bar{\varepsilon}_p^f} (\sigma_m / \bar{\sigma})\, d\bar{\varepsilon}_p$ and $\bar{\varepsilon}_p^f$ is

plotted for all failed locations to calculate the material constants *A* and *B*.

To set the final workability limit, the trend passing through the plotted points is lowered vertically to keep all the failure points above it. This final workability limit acts as a lower boundary separating the failure zone from the no failure zone which can be used in the CH design and optimization processes. The slope of this linear relationship is given by the *A* parameter while the material constant *B* is the intersection of the ordinate and this line. This final workability limit acts as a lower boundary separating the failure zone from the no failure zone and can be used in CH design and optimization processes. The final result of the universal workability criterion is shown in Fig. 8.

The final form of the universal workability criterion is:

$$\bar{\varepsilon}^f = 1.48 - -0.31 \int_0^{\bar{\varepsilon}^f} \frac{\sigma_m}{\bar{\sigma}} d\bar{\varepsilon}$$

VI. CONCLUSION

A new technique to set a universal workability criterion for predicting the limits for internal and external ductile fracture in cold-headed steel parts is presented with an experimental and finite element simulation methodology. This methodology consists of the DWCT to simulate the CHP in conjunction with metallographic inspection and finite element analyses (implemented within ABAQUS/Explicit) and has been applied to determine the workability limits for 1038 steel in CHP.

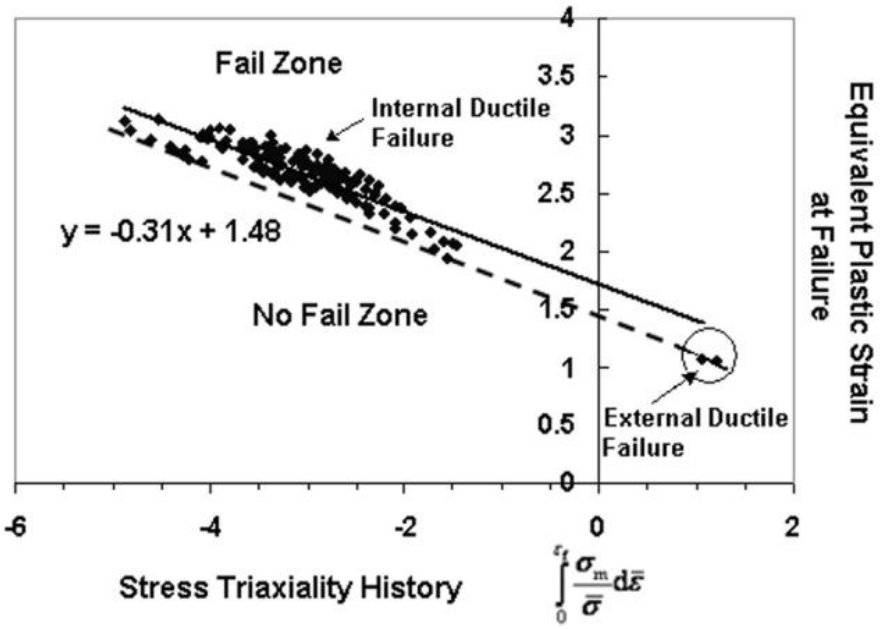


Fig. 8 Preliminary result of the universal ductile failure workability limits of the internal and external ductile failure using the stress triaxiality history criterion

This encouraging result provides a strong motivation to conduct experimental and FE studies on other materials using this new universal workability criterion for internal and external failure using the same methodologies employed in this study.

REFERENCES

[1] A. Sabih, and J. A. Nemes, "Experimental and finite element simulation study of the adiabatic shear band phenomenon in cold heading process," Journal of Materials Processing Technology, 212 (5), pp. 1089–1105, May 2012

[2] T. Okamoto, T. Fukuda, T. and H. Hagita, "Material fracture in cold forging- systematic classification of working methods and types of cracking in cold forging," The Sumitomo Search, 9, pp. 216-227, 1973.

[3] N. Nickoletopoulos, M. Hone, P. Wanjara, P., Y. Verreman, J. A. Nemes, J. J. Jonase, and S. Yue, "Development of a fracture criterion for cold heading," Wire Journal International, 34(9), pp. 90-98, 2001.

[4] H. Kudo, K. Sato, and K. Aoi, "On Cold Forgeability Test," CIRP Annals. vol. 16, pp. 309-318, 1968.

[5] C. Levaillant, "Ductilité, plasticité et mise en forme de métaux," In Tome I, Chapter H (Eds.), Centre de mise en forme des matériaux (CEMEF) (pp.H1-H25). Paris, France, 1986.

[6] S. L. Semiatin, and G. D. Lahoti, "The occurrence of shear bands in metalworking," In Mescall, J. and Weiss, V. (Eds.), Material behavior under high stress and ultrahigh loading rates, Sagamore Army Materials Research Conference (pp. 119-159). Lake Placid. N.Y, 1982.

[7] T. W. Wright, "The physics and mathematics of adiabatic shear bands" Cambridge monographs on mechanics. Cambridge University Press, 2002.

[8] J. R. Klepaczko, P. Lipinski, and A. Molinari, "An Analysis of the Thermoplastic Catastrophic Shear in Some Metals," DGM Informations Gesellschaft MBH, Impact Loading and Dynamic Behavior of Materials, 2, pp. 695-704, 1988.

[9] J. R. Klepaczko, and B. Rezaig, "A numerical study of adiabatic shear banding in mild steel by dislocation mechanics based constitutive relations," Mechanics of Materials, 24(2), pp. 125-139, 1996.

[10] S. Lee, K-M Cho, C. S. Lee, and W. Y. Choo, "Microstructural study of adiabatic shear band formed by ballistic impact in AN HY-100 steel," Metallurgical and Material transactions Series A, 24(10), pp. 2217-2224, 1993.

[11] M. Nabil Basim, "Study of the formation of adiabatic shear bands in steels," Journal of Material Processing Technology, 119, pp. 234-236, 2001.
[12] J. Kalthoff, and S.Winkler, "Failure mode transition at high rates of loading," In Chiem, C. Y., Kunze, H. D., Meyer, L. W., (Eds.), Proceedings of the International Conference on Impact Loading and Dynamic Behaviour of Materials (pp. 43-56). Deutsche Gesellschaft fur Metallkunde, 1988.
[13] H. C. Rogers, "Adiabatic shearing- general nature and material aspects," In Mescall, J. and Weiss, V. (Eds.), Material behavior under high stress and ultrahigh loading rates. Sagamore Army, Materials Research Conference (pp. 101-118). Lake Placid. N.Y., 1983.
[14] P. W. Lee, and H.A. Kuhn, "Upset Testing, Workability Testing Techniques, American Society for Metals (ASM)," Metals Park, Ohio, Chapter 3, pp. 37-50, 1984.
[15] M. G. Cockroft, and D. J. Latham, "Ductile and workability of metals," J. Inst. Met., 96, pp. 33¯39, 1968.
[16] L. Daridon, O. Oussouaddi, and S. Ahzi, "Influence of the material constitutive models on the adiabatic shear band spacing: MTS, power law and Johnson–Cook models," International Journal of Solids and Structures, 41(11-12), pp. 3109-3124, 2004.
[17] S. L. Venugopal, Y. V. Mannan and R. K. Prasad, "Instability map for cold and warm working of as-cast 304 stainless steel," Journal of Materials Processing Technology, 65(1-3), pp. 107-115, 1997.
[18] S. P. Timothy, " The structure of adiabatic shear bands in metals: a critical review," Acta Metallurgica, 35(2), pp. 301-306, 1987.
[19] A. Sabih, and J. A. Nemes, "Internal ductile failure mechanisms in steel cold heading process," Journal of Materials Processing Technology, Journal of Materials Processing Tech. (May 2009), 209 (9), pp. 4292-4311, 2009.
[20] A. Sabih, P. Wanjara, and J. A. Nemes, "Characterization of internal voids and cracks in cold heading of dual phase steel," ISIJ Int. 45 (8), pp. 1179-1186, 2005.
[21] A. Sabih, J. A. Nemes, N. Nickoletopoulos, and M. Hone, "A workability criterion for internal ductile fracture in the steel cold heading process," Wire J. Int. 39 (3), pp. 155-159, 2006.
[22] R. Hambli, "Finite Element Simulation of fine blanking processes using a pressure-dependent damage model," Journal of Materials Processing Technology, 116(2-3, 24), pp. 252-264, 2001.
[23] B. P. P. A. Gouveia, J. M. C. Rodrigues, and, P. A. F. Martins, "Ductile fracture in metalworking experimental and theoretical research, " Journal of Materials Processing Technology, 101, pp. 52-63, 2000.
[24] R. Shivpuri, S. Babu, S. Kini, P. Pauskar, and A. Deshpande, "Recent advances in cold and warm forging process modeling techniques: selected examples," Journal of Materials Processing Technology, 46, pp. 253-274, 1994.
[25] M. Oyane, "Criteria of Ductile Fracture Strain," Bull. Japan Soc. Mech. Eng., 15, (90), pp. 1507-1513, 1972.
[26] M. Oyane, T. Sato, K. Okimoto, and S. Shima, "Criteria for Ductile Fracture and their Applications," Journal of Mechanical Working and Technology, 4, pp. 65-81, 1980.
[27] Y. Shin, and K. Kawai, "A study of optimum die-design in the heading process with two blows. Part 1: Experimental study," Journal of Materials Processing Technology, 28(3), pp. 391-406, 1991.
[28] Y. Shin, and K. Kawai, "A study of optimum die-design in the heading process with two blows. Part 2: Use of finite-element analysis," Journal of Materials Processing Technology, 30(1), pp. 67-77, 1992.
[29] F. D. Fischer, O. Kolednik, G. X. Shan, and F. G. Rammerstorfer, "A Note on Calibration of Ductile Failure Damage Indicators," International Journal of Fracture, 73, pp. 345–357, 1995.
[30] G. R. Johnson, and W. H. Cook, "A constitutive model and data for metals subjected to large strains, high strain rates and high temperatures," In Proceedings of the Seventh International Symposium on Ballistic (pp. 541-547). The Hague, Netherland, 1983.
[31] M. A. Meyers, G. Subhash, B. K. Kad, and L. Prasad, "Evolution of microstructure and shear-band formation in α-hcp titanium," Mechanics of Materials, 17(2-3), pp. 175-193, 1994.
[32] R. C. Batra, and B. M. Love, "Consideration of microstructural effects in the analysis of adiabatic shear bands in a tungsten heavy alloy," International Journal of Plasticity, 22, pp. 1858-1878, 2006.
[33] H. Kolsky, "An investigation of the mechanical properties of materials at very high rates of loading," In Proceeding of the Physical Societ, section B. London, 62, pp. 676-700, 1949.

★★★